Non-linear dynamic stability analyses of a lined geomembrane rock fill dam

J.L. Castillo
Ausenco, Denver, CO, USA

ABSTRACT: This paper presents a non-linear dynamic analyses for a geomembrane lined large rock fill dam located in a high seismicity zone in South America. The analysis considered dam configuration of 120 m high. The embankment will be constructed primarily of rock fill material in a downstream fashion. The geomembrane will be lined along the dam upstream slope face and extend along impoundment. A thin zone behind upstream face and uppermost portion of the dam will be constructed with glacial moraine earth fill. Lower upstream slope will be buttressed with alluvium fill. The dynamic analyses were conducted as non-linear two-dimensional analyses using the Fast Lagrangian Analysis of Continua (*FLAC*) computer code. Seismic performance of the embankment was evaluated employing UBCHYST constitutive model, nonlinear hysteretic damping for predicting its permanent deformations of the dam of subject to design earthquake peak ground acceleration intensity and duration. Results of the dynamic analyses indicate that the geomembrane lined rockfill dam is stable under the Maximum Credible Earthquake (MCE) magnitude Mw 9.5 considered in the design. Discussions of the analysis results including the tensile forces of the geomembrane and relative displacements at the geomembrane-alluvium interface are also presented for the assessment of the geomembrane integrity at different applied tailings loads under the design earthquake.

1 INTRODUCTION

A downstream rockfill dam was designed for new tailings storage facility (TSF) located in a high seismicity zone in South America. This technical paper presents the results of dynamic stability analyses of the dam. The analyses considered two cases corresponding to the starter dam (Stage 1) and ultimate dam (Stage 7) configurations. The tailings dam will be constructed on a dense foundation soil consisting of a glacial moraine underlain by bedrock. The bedrock is located at depths ranging from 25 to 30 m below a prepared foundation grade.

The tailings dam at Stage 1 and Stage 7 will be 56 m and 120 m high (measured at center line), respectively. The embankment will be constructed primarily of rockfill materials in a downstream fashion. The geomembrane will be lined along the upstream slope face and extend along the impoundment upstream area. A thin zone behind the upstream face of the dam will be constructed with glacial moraine earth fill. The upstream slope will be faced with alluvium and also buttressed at the toe with alluvium. The downstream and upstream slopes of the embankment will be on the order of 1.5H:1V and 2H:1V, respectively. Cross section of the Stage 1 and Stage 7 dam for the modeling is shown on Figure 1.

A dynamic analysis was performed using an advanced non-linear constitutive model to be implemented in *FLAC* (Fast Lagrangian Analysis of Continua) finite difference computer code (Itasca 2004). The *FLAC* code solves the equations of motion in explicit form in the time domain using very small time steps and incorporates non-linear inelastic stress-strain soil behavior.

A hysteretic damping model for nonlinear soil behavior during dynamic loading was incorporated into *FLAC* where the material damping and tangent modulus are modeled as a function of

the level of stress and strain in each point in time and space. The material damping was modeled using a hysteretic damping subroutine developed by Professor Peter Byrne at the University of British Columbia (Byrne 2005, Naesgaard & Byrne 2011).

The procedures adopted for the static and dynamic analysis, input parameters, earthquake time-history records selection and results of the analyses are summarized in the following sections.

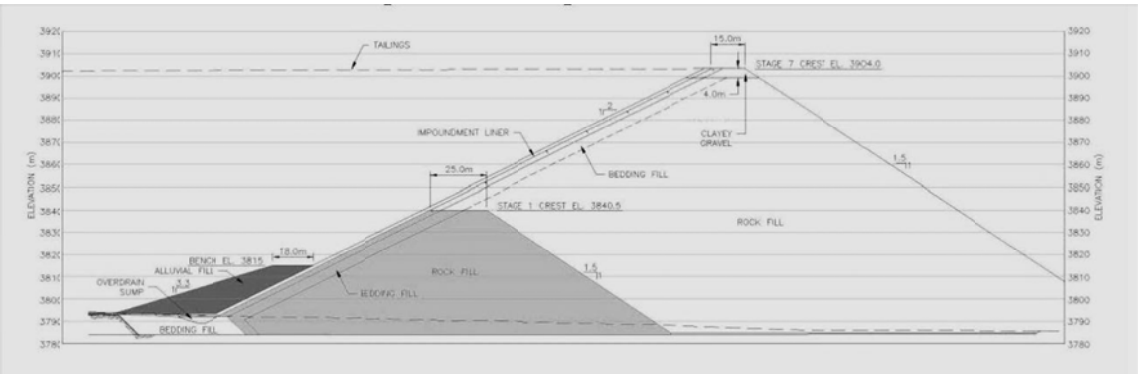

Figure 1. Tailings dam section for Stage 1 and Stage 7.

2 MATERIAL PROPERTIES

For the static analyses the dam fill properties were modeled using linear behavior in order to simplify the model. The analysis incorporates Mohr-Coulomb failure criterion. Effective stress properties were utilized for the analysis.

The soil and rock fill properties adopted were based on the values obtained from laboratory testing, published literature and previous experience with similar materials (Hunter et al. 2003, Kulhawy 1998). The parameters adopted for use in the static analysis are given in Table 1.

Table 1. Material properties for static analysis.

Material	Density KN/m^3	Elastic Properties		Mohr Coulomb	
		Bulk Modulus (MPa)	Shear Modulus (MPa)	Cohesion (kPa)	Friction angle
Rockfill	20.0	75.0	34.6	0	Varies[(1)]
Alluvial/Moraine fill	21.9	50.0	23.1	0	38
Foundation-Moraine	23.2	45.5	23.4	0	40
Tailings	17.3	It was modeled as heavy liquid			

[(1)] The friction angle is a function of the effective normal stress (Leps 1970).

For dynamic analysis of the Stage 7 dam, the tailings were assumed to fully liquefy and were modeled as an applied pressure to the upstream face of the dam. This neglects the shear strength of the tailings prior to the onset of liquefaction as well as the nominal post-liquefaction shear strength and adds conservatism to the results. This simplifying assumption was made to avoid adding an excessive number of elements in the model that would increase computational time.

As the *FLAC* model for the Stage 1 configuration was significantly smaller than the Stage 7, the liquefied tailings were modeled as elements with a residual post-liquefaction strength to effective overburden pressure ratio of 0.15 (i.e. Su/p'=0.15). Modeling the tailings in this manner

also allowed the behavior of the geomembrane liner and geomembrane-alluvium interface to be placed in the upstream portion of the tailings dam.

The geomembrane was modeled with beam elements, taking into account both behavior of the flexible fabric and interaction with the soils right above and below it. By assigning a zero moment of inertia to the beam, it acts like a flexible member that provides no moment resistance. Interface material properties was modeled to control a sliding along the interface between the geomembrane and its adjacent soils.

3 NUMERICAL MODELING APPROACH

The static analyses were conducted using the *FLAC* code primarily to establish the state of stress following construction sequences prior to earthquake loading. This was done to determine the pre-earthquake stress conditions within the embankment.

The mesh size for the *FLAC* model was selected to provide accurate seismic wave transmission. The model meshes for the Stage 1 and Stage 7 geometries are shown in Figures 2 and 3. The earth-filled buttress at upstream toe of the dam was assumed to be fully saturated. Based on an assumption was made that the liner system will function effectively and little seepage would occur through the body of the dam, indicating the embankment body is in unsaturated conditions. Although groundwater level is on the order of 10 to 20 m deep below the prepared foundation grade and the impoundment area will be fully lined with the geomembrane to minimize pond water discharge into the foundation, the foundation material was conservatively considered as fully saturated.

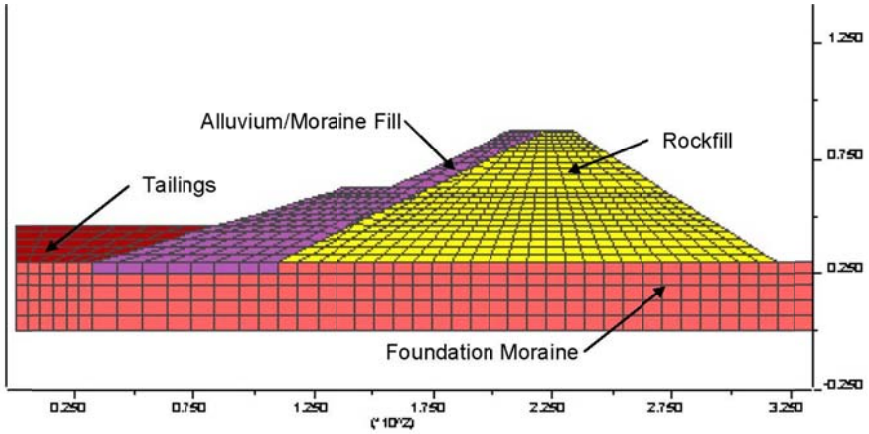

Figure 2. Model mesh – Stage 1.

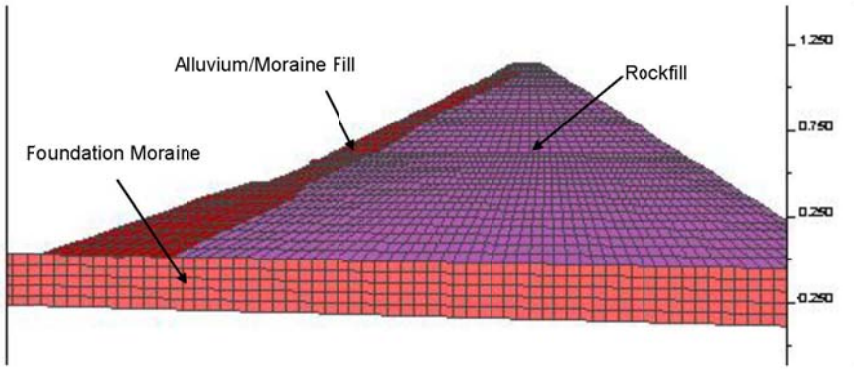

Figure 3. Modeled mesh – Stage 7.

3.1 *Damping*

Dynamic response of earth and rock fill structures is very dependent on an amount of energy internally dissipated through the fills during shaking. This mechanism of energy dissipation is commonly referred to as "damping". The magnitude of the damping is reflected in, and is proportional to, the "area" enclosed by the stress-strain hysteresis loop for a complete loading-unloading cycle, which in turn depends on the fill type, and increases with the level of shear strain.

There are two basic approaches to model or incorporate damping in dynamic analyses: 1) equivalent viscous damping, and 2) hysteretic damping. A system in which the damping at any instant is proportional to the velocity of motion is said to possess viscous damping. This model does not produce realistic response of earth structures, nor does it account for the permanent displacement due to the inelastic behavior of the material. In a hysteretic damping model, damping is proportional to displacement, but in phase with the velocity. For seismic loading of earth structures, a hysteretic model of damping seems to be more realistic. Accordingly, for the current analysis, the hysteretic damping approach was adopted by incorporating into *FLAC*, a hysteretic damping subroutine UBCHYST developed at the University of British Columbia (Byrne 2005, Naesgaard & Byrne 2011). The UBCHYST is applicable to highly permeable granular soils and non-saturated granular soils.

The UBCHYST subroutine allows for modeling the nonlinear and inelastic stress-strain response of soil directly in the dynamic analyses. This is achieved by treating the material damping and tangent modulus as a function of the level of stress and strain reached at each point in the time and space, and keeping track of whether the loading or unloading take place. Such response, including the phenomenon of "size of stress-strain hysteretic loops vary with strain level", is very similar to that observed at relatively low strain levels (e.g. 0.0001 to 0.01 percent strain) during laboratory cyclic loading testing, and a small amount of viscous damping, generally in the range of 1 to 2 percent, is added to match the measured response.

3.2 *Shear modulus*

In general, the secant shear modulus is defined in terms of the small-strain amplitude shear modulus (G_{max}) and the variations of normalized shear modulus at any strain level (G_{sec}/G_{max}) with the shear strain amplitude. The secant shear modulus decreases as the shear strain amplitudes increase.

The shear modulus is strongly influenced by three main factors: 1) the confining pressure, 2) the strain amplitude, and 3) the void ratio. An empirical, but convenient relationship between the shear modulus and the confining pressure for cohesionless soils, as given in Equation 1 (Seed & Idriss 1970) below, was used in the dynamic analysis:

$$G_{max} = 21.7K_{2,max} * Pa * \left(\sigma'_m\right)^{1/2} \quad (1)$$

Where, the mean effective confining stress σ'_m and the maximum Shear Modulus G_{max} are in kPa (kilo Pascal) unit, and the influence of the void ratio and the strain amplitude is reflected in the

soil modulus coefficient $K_{2,max}$. According to Byrne (2005) for loose and dense rock fill, the value of $K_{2,max}$ varies from 100 to 160. In the dynamic analysis of the rock fill tailings dam, a $K_{2,max}$ value of 140 was adopted for the compacted rock fill.

3.3 *Model calibration*

The hysteretic damping model was calibrated to match the laboratory test data for gravel and rock fill using a single element simulation in *FLAC*. Due to the large diameter of the test specimens and expensive laboratory facility required, there are limited investigations of the shear modulus and damping ratios presented in the form of the stress-strain loops for coarse gravel and rock fill materials. Hence, an indirect method of model calibration and verification for gravel and rock fill materials has been adopted. Stress-strain loops for gravel and rock fill were produced using a simple hysteretic total-stress constitutive model (UBCHYST). The hysteretic damping model calculates the tangent shear modulus (G_t) as a function of the peak shear modulus (G_{max}) multiplied by a reduction factor that is a function of the developed stress ratio and the change in stress ratio to reach each failure (Naesgaard & Byrne 2011).

It is not practical to compare the rock fill stress-strain loops calculated by *FLAC* to stress-strain loops obtained from laboratory testing due to the laboratory limitations in testing a rock fill material including large rock fragments. In order to calibrate the model G_{sec}/G_{max} and damping, calculations from the stress-strain loops were compared to curves commonly used for either equivalent viscous damping or equivalent linear approach published in the technical literature.

A summary of the hysteretic damping model calibration and the published data for rock fill and gravelly soils are shown in Figures 4 and 5. The model was run for the cases where the tangent shear modulus is calculated with exponents of both 2 and 3.

The predicted hysteretic model modulus degradation curves provide a reasonable fit to the published modulus data as an exponent of 2 is employed. Damping calculated using the hysteretic model does not provide a good match to the published damping versus shear strain curves for coarse alluvial soils from laboratory testing and the curves suggested for rockfill (Gazetas 1992). However, the calculated damping appears to provide a favorable match to the damping values back-calculated from actual measurements of rockfill embankment response during earthquakes (Iwashita et. al. 1995).

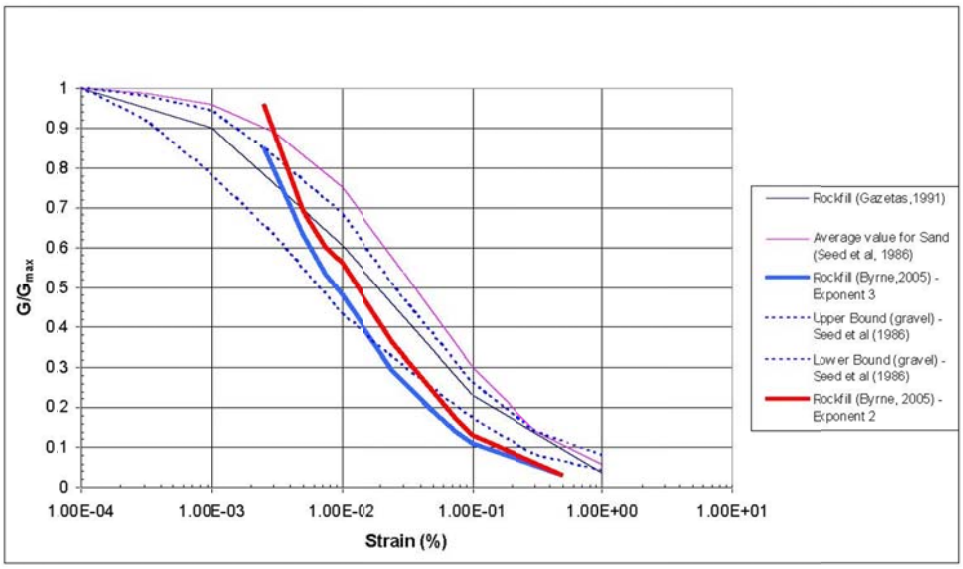

Figure 4. G_{sec}/G_{max} modulus reduction vs. cyclic shear strain curves.

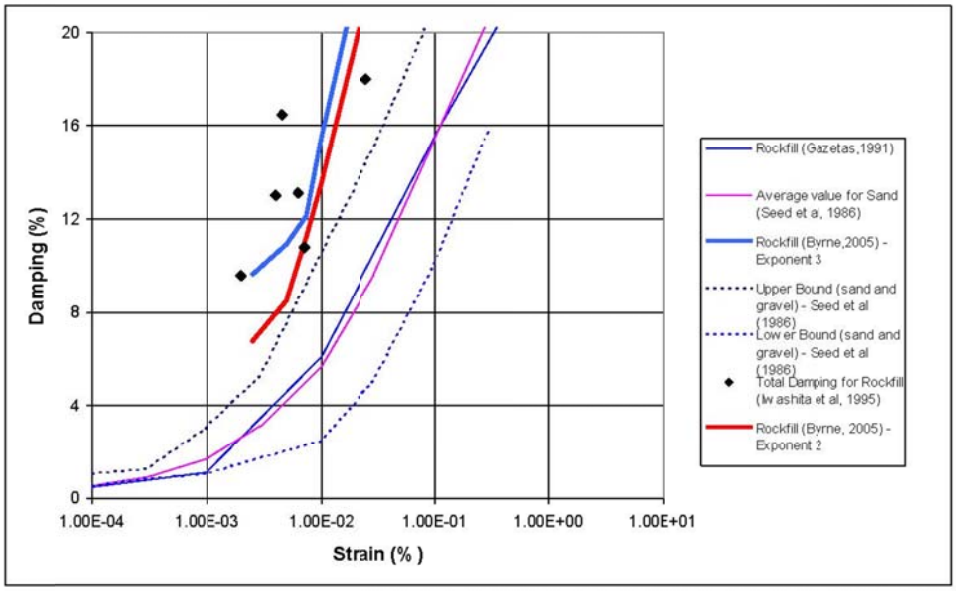

Figure 5. Damping vs. cyclic shear strain curves.

3.4 *Earthquake ground motion*

The controlling MCE for the dynamic analysis was assumed to be a large magnitude megathrust event (Mw 9.5) resulting in 0.25 g peak horizontal ground acceleration.

For the dynamic analysis a suite of three or more earthquake time-histories that correspond to the design earthquake are required as the input ground motion. For the reason, these records should be selected on the basis of the duration of the event, tectonic setting (subduction zone thrust faulting versus shallow crustal faults), source-to-site distance, frequency content, and local site conditions. In general, a suite of earthquake time-histories selected on the above-mentioned basis are used to impart some sort of randomness to the input ground motion and avoid potential bias in the results due particularly to any one of those time-histories.

A total of five earthquake time-histories were selected, modified in the frequency domain to obtain a better fit to the spectra design, and applied to the model as the seismic loads for the dynamic response analyses of the dam.

4 RESULTS AND FINDINGS

4.1 *Dam Stage 7*

The displacement experienced in the horizontal and vertical directions as well as the peak acceleration generated at several points within the model were measured for each trial performed. The upstream crest, mid-crest and downstream crest of the dam were monitored throughout all the trials for the displacement under the seismic loading conditions. The results of each trial are summarized in Table 2.

Table 2. Embankment seismic response.

			Peak Accel. (g)		u/s-Crest Displacement (m)		Mid-Crest Displacement (m)		d/s-Crest Displacement (m)	
Earthquake	Station	Comp	Mid-height Dam	Mid-Crest	X Disp	Y Disp	X Disp	Y Disp	X Disp	Y Disp
Ocoña (Peru) 06/23/01	Moquegua	EW	0.42	1.10	1.80	0.72	2.20	0.75	3.82	2.09
		NS	0.44	1.07	2.30	0.49	2.56	0.68	3.60	1.58
Lima 10/03/74	Parque Res.	EW	0.49	0.97	1.30	0.62	1.80	0.70	2.90	1.68

Valp. (Chile)	Papudo	140	0.40	1.05	0.62	0.40	0.87	0.37	2.40	1.76
03/03/85	Pichilemu	EW	0.55	1.09	2.02	0.34	2.20	0.47	3.08	1.29
Average			0.46	1.06	1.61	0.51	1.93	0.59	3.16	1.68
Minimum			0.40	0.97	0.62	0.34	0.87	0.37	2.40	1.29
Maximum			0.55	1.10	2.30	0.72	2.56	0.75	3.82	2.09

d/s – downstream u/s – upstream

For the five earthquake time-history records considered in this study, the maximum vertical displacements at the upstream edge, mid crest and downstream edge of the dam crest are approximately 0.72 m, 0.75 m and 2.09 m, respectively. Based on the empirical approach for estimating earthquake induced settlements developed by Swaisgood (2003), the vertical displacement for the tailings dam was estimated to be approximately 0.60 m after the earthquake event. This is consistent with the vertical displacement at upstream edge of the dam crest calculated by *FLAC* where the value is 0.72 m. The dam has sufficient freeboard (1 m) to avoid loss of containment although slight damage to the structure would be induced. As the free water pool within the tailings impoundment will be maintained a minimum distance of 500 m from the dam at all times with tailings beach developed between the dam and water pool, no releases would occur for the level of deformations indicated by the *FLAC* model.

Figures 6a and 6b depict the pattern of deformation. These figures depict the results for the modified Moquegua EW time-history which has the highest energy content and largest displacements. The dynamic response for the other seismic records exhibit a similar pattern.

These results demonstrate that the Stage 7 tailings dam is stable at the seismic loading considered for the megathrust subduction zone interplate MCE of Mw = 9.5. Permanent displacements of the dam crest are consistent with empirical data and there are no failures compromising the global dam stability.

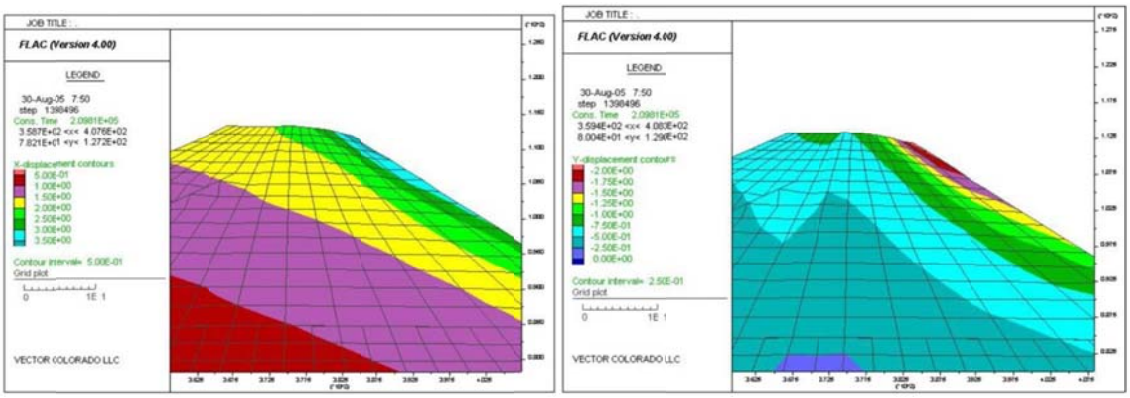

(a) (b)

Figures 6. (a) Horizontal displacements – Moq. EW. (b) Vertical displacements – Moq. EW.

4.2 *Dam Stage 1*

Although the Stage 1 tailings dam will have a very short exposure period prior to construction of the next stage (less than 24 months), the dynamic analysis for this stage was performed considering the MCE seismic loading as well. Since the modified Moquegua EW record has the highest energy content and resulted in the largest displacements for the Stage 7 dam, this time-history was used for the dynamic analysis of the tailings dam Stage 1. This analysis was conducted to assess relative displacements along the geomembrane liner interface, and axial tensile force in the geomembrane.

Four (4) different scenarios for upstream tailings loading conditions were analyzed, as shown in Figure 7, to determinate a case to produce the largest relative displacements along the liner interface. The tailings were considered to be saturated and fully liquefy under the earthquake load-

ing. The tailings were modeled with an undrained residual strength throughout the *FLAC* runs at an attempt to conservatively model the tailings as being liquefied at the onset of the earthquake rather than at some point during the shaking.

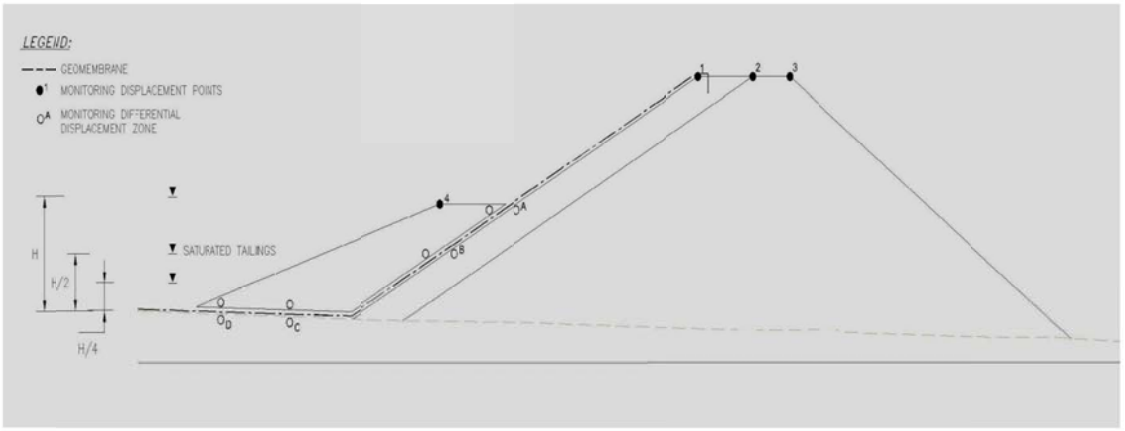

Figure 7. Displacement monitoring point locations & upstream tailings levels considered.

Structural beam elements were used to model the geomembrane. The beam elements drastically affect the time step of the model during the dynamic calculation. Hence, these beam elements were not considered initially to determine critical upstream tailing loading and only interface properties representing frictional behavior between the geomembrane and adjacent soils were used. For the critical upstream tailings loading condition only, the beam elements (geomembrane) were fully incorporated to evaluate integrity of the liner following the earthquake. This critical loading condition will exist for only a very short period of time until more tailings are deposited. This will be able to significantly reduce the risk for occurrence of the conditions considered.

The seismic dam response for the four (4) scenarios for upstream tailings level are shown in Table 3.

Table 3. Relative displacements along the liner interface (m).

	Interface-Upper (Zone A)			Interface-Middle (Zone B)			Interface-mid-Bottom (Zone C)		Interface-Left-Bottom (Zone D)	
Upstream Loads	X Disp	Y Disp	Relative Interface Displac.	X Disp	Y Disp	Relative Interface Displac.	X Disp	Y Disp	X Disp	Y Disp
H	0.25	0.12	0.28	0.61	0.31	0.68	0.09	0.01	0.31	0.05
H/2	0.56	0.29	0.63	0.77	0.39	0.86	0.36	0.01	0.75	0.05
H/4	0.40	0.19	0.44	0.56	0.28	0.63	0.34	0.01	1.35	0.02
No tailings	0.40	0.20	0.45	0.59	0.28	0.65	0.11	0.02	1.31	0.01

Note: See Figure 7 for monitoring relative displacements zones location.

The maximum relative displacement in the inclined liner interface is 0.86 m and occurs around zone B (see Fig. 7) as the tailings level is at the mid-height of the alluvial buttress fill (H/2). The upstream tailings loading at mid height of the alluvial fill is also the most critical upstream loading scenario (as shown in Table 3) due mainly to saturation of the lower half of the alluvial fill by the tailings. This scenario exhibits the largest displacement for the overall alluvial fill buttress, where the edge of the alluvial buttress crest (Point 4) is displaced 1.07 m horizontally and 0.40 m vertically. As previously noted, these results assume that the tailings would liquefy at the onset of the earthquake where in reality liquefaction would not be triggered until sometime later during the earthquake ground motion and the displacements would be less.

The *FLAC* model results indicate a local large relative displacement around Zone D which ranges from 1.31 to 1.35 m when very low tailings height (H/4) and no tailings are applied at the

upstream slope, respectively. These scenarios are not considered critical since the displacements happen locally with very low normal stress.

Once the critical upstream tailings loading was identified, the model was run considering the geomembrane as structural beam elements and the interface with the soils above and below the geomembrane. The resulting seismic response of the dam is summarized in Table 4. The maximum relative displacement between the alluvial fill and the rockfill dam is 0.89 m located at the mid-height of the inclined interface (Zone B).

The axial force in the geomembrane and the shear stress were monitored during the seismic loading. A typical force distribution in the inclined liner is shown in Figure 8, where the tensile force occurs in the upper zone (Zone A). The maximum tensile axial force in the geomembrane was 6.5 N/mm which is 31 percent of the tensile break strength (21 N/mm) specified for the geomembrane.

Table 4. Relative displacements along the liner interface (m) for tailings at mid-height.

	Interface-Upper (Zone A)			Interface-Middle (Zone B)			Interface-mid-Bottom (Zone C)		Interface-Left-Bottom (Zone D)	
Upstream Loads	X Disp	Y Disp	Relative Interface Displac.	X Disp	Y Disp	Relative Interface Displac.	X Disp	Y Disp	X Disp	Y Disp
Tailings Mid-Height (H/2)	0.60	0.33	0.68	0.80	0.40	0.89	0.55	0.03	0.42	0.00

Note: See Figure 7 for monitoring relative displacements zones location.

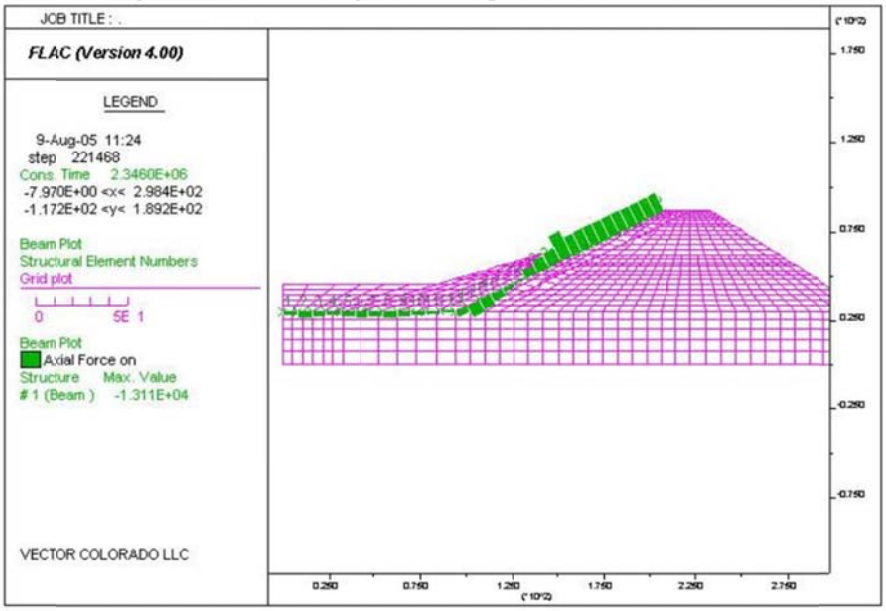

Figure 8. Axial force in the geomembrane.

5 CONCLUSIONS

In order to assess the potential effects of strong earthquake on the tailings dam a nonlinear analysis procedures were employed to model the pattern of permanent inelastic deformation resulting from high levels of ground motion. The analyses adopted the earthquake loading conditions for the design MCE with the largest peak ground acceleration as well as the MCE with the highest energy content, longest duration and damage potential.

The results demonstrate that the Stage 7 tailings dam will be stable at the seismic loading considered for the megathrust subduction zone interplate MCE of Mw = 9.5 earthquake directly beneath the tailings dam site. Permanent displacements of the dam crest are consistent with empirical data and there are no failures compromising the global dam stability. However, the level of deformation indicates that some cracking and slumping at the edge of the embankment crest could occur but that designed freeboard would remain adequate in preventing uncontrolled re-

lease of tailings or water from within the impoundment. These results are consistent with ICOLD guidelines (Wieland 2005) which indicate that "significant structural damage is accepted" for MCE ground motions although no uncontrolled release form the reservoir shall occur.

Additionally, the geomembrane installed on the upstream slope of the Stage 1 dam and extended into the impoundment will be sustainable to the design earthquake without damage. The maximum tensile axial force generated within the geomembrane occurred in the upper zone due to the relative displacement between the geomembrane and alluvial buttress/ tailings and was estimated to be approximately 31% of the allowed tensile break strength specified for the geomembrane.

REFERENCES

Byrne, P. 2005. Professor Emeritus at the University of British Columbia, Civil Engineering Department. Personal communication.

Gazetas, G. & Dakoulas, P. 1992. Seismic analysis and design of rockfill dams: state-of-the-art. *Soil Dynamics and Earthquake Engineering* Vol. 11 pp. 27-61.

Hunter G. & R. Fell. 2003. Rockfill Modulus and Settlement of Concrete Face Rockfill Dams. *Journal of Geotechnical and Geoenvironmental Engineering*.

Itasca Consulting Group, Inc. 2004. *FLAC – Fast Lagrangian Analysis of Continua, Version 4.0 User's Manual*. Minneapolis: Itasca.

Iwashita, T. et al. 1995. Dynamic Deformation Characteristics of Rockfill Materials from Laboratory Test, In-Situ Test and Earthquake Motion Analysis. In *Proceedings of the 3rd International Conference on Recent Advances in Geotechnical Earthquake Engineering and Soil Dynamics, St. Louis, Missouri, April 2-7*.

Kulhawy, F. 1998. *Manual on Estimating Soils Properties for Foundation Design*. Prepared for Electric Power Research Institute. Research Report 1493-8.

Leps, T.M. 1970. Review of Shearing Strength of Rockfill. *Journal of Soil Mechanics and Foundations Division, ASCE* 96(SM4): 1159-1170, July 1970.

Naesgaard, E. & Byrne, P. 2011. *Hysteretic Model for Non-liquefiable Soils (UBCHYST5d)*. UBCHYST5d Memo.

Seed, H. B. & Idriss, I. M. 1970. *Soil moduli and damping factors for dynamic response analysis*. Report No EERC 70-10, Earthquake Engineering Research Center, University of California, Berkeley, California.

Swaisgood, J.R. 2003. Embankment dam deformations caused by earthquakes. In *Proc., Pacific Conference on Earthquake Engineering. Christchurch, New Zealand*: Paper No.014

Wieland, M. 2005. Review of seismic Design Criteria of Large Concrete and Embankment Dams. Presented at the *73rd Annual Meeting of ICOLD, Tehran, Iran, May 1-6*, Paper No. 012-W4.